Supporting Information: Cofactor-mediated conformational dynamics promote product release from *E. coli* dihydrofolate reductase via an allosteric pathway

David Oyen, R. Bryn Fenwick, Robyn L. Stanfield, H. Jane Dyson and Peter E. Wright*

Department of Integrative Structural and Computational Biology and Skaggs Institute for Chemical Biology, The Scripps Research Institute, 10550 North Torrey Pines Road, La Jolla, California 92037, United States.

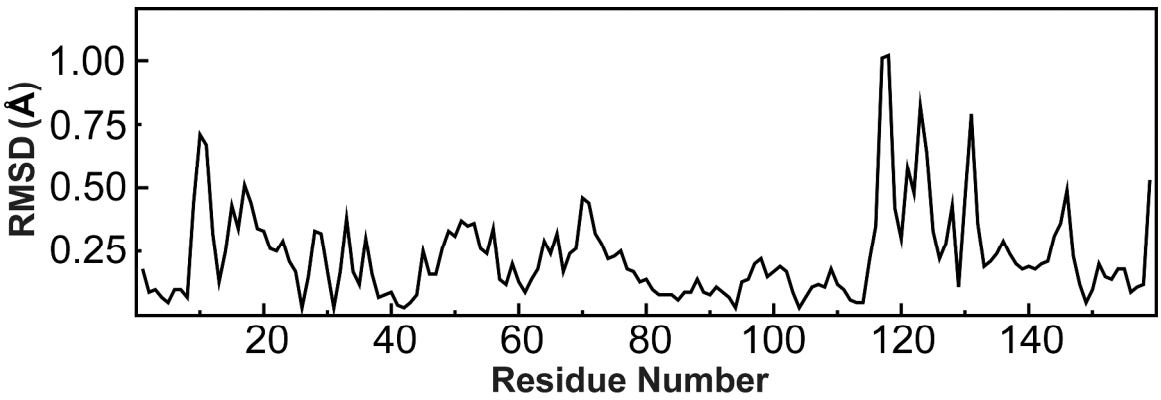

Figure S1. The C_α main-chain coordinate RMSDs between the WT and L28F E:ddTHF:$NADP^+$ crystal structures plotted as a function of the residue number. The largest deviation is seen for residues 120-130, because of the poorer electron density in that region. The RMSD between the structures is very small, indicating minimal structural perturbation of the backbone upon mutation.

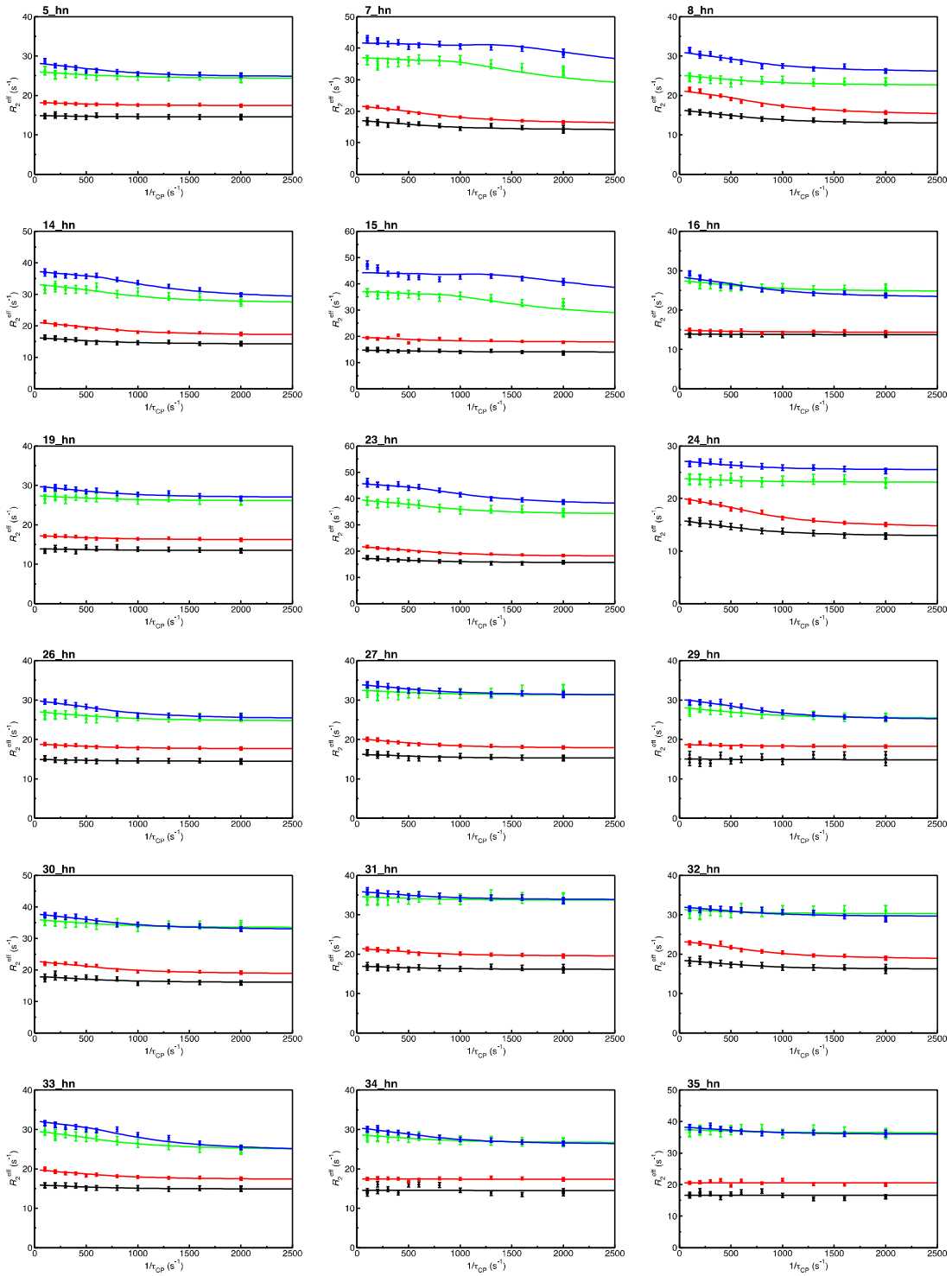

Figure S2. R_2 relaxation dispersion profiles for the WT E:THF:NADPH complex at 300 K, pH 7.6. Black and red, amide ^{15}N dispersion data at 11.7 and 18.8 T, respectively. Green and blue, amide ^{1}H dispersion data at 11.7 (500 MHz) and 18.8 T (800 MHz), respectively. Solid lines indicate the best fit of the data to a global two-site exchange model.

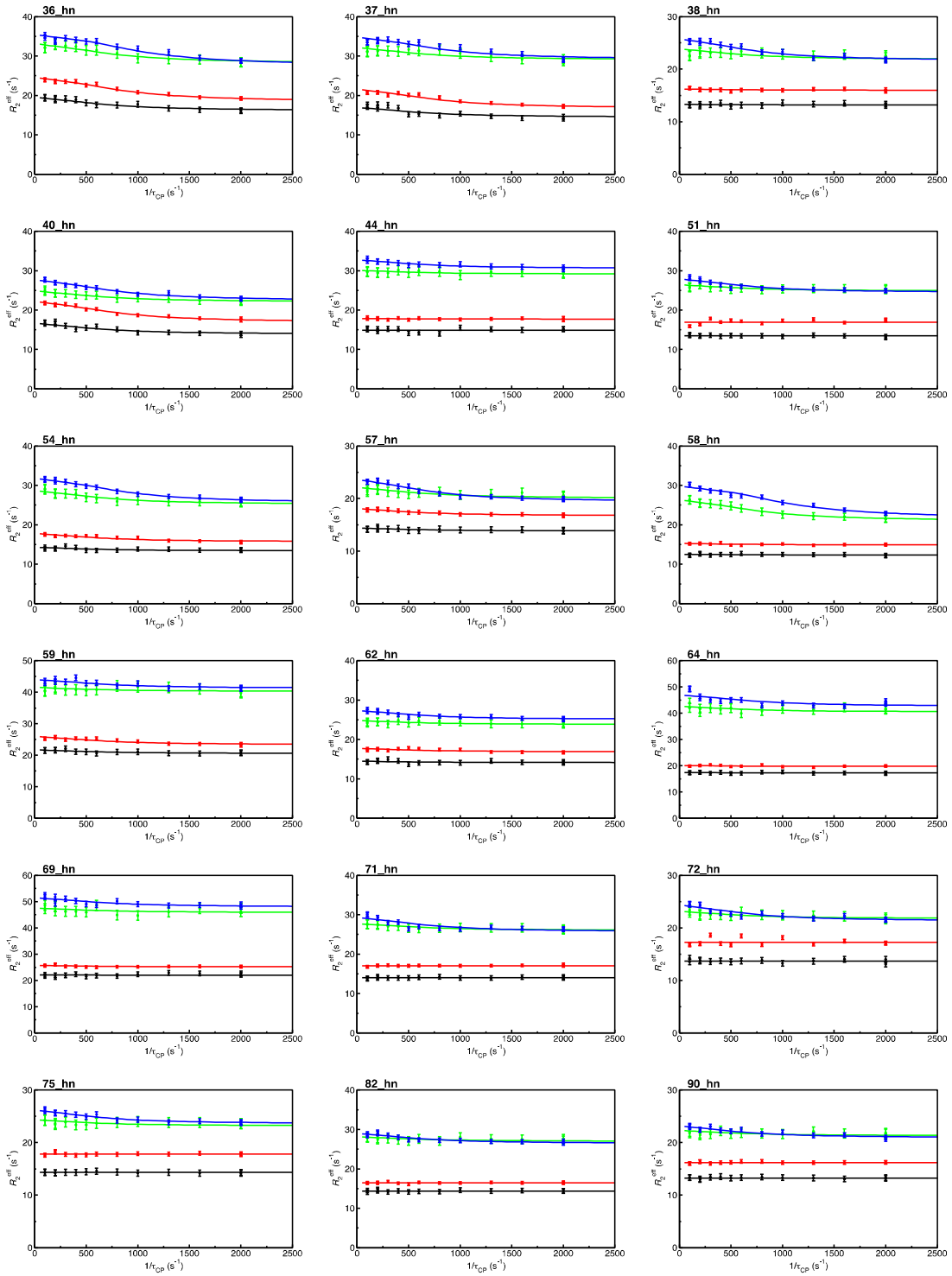

Figure S2 (Continued). R_2 relaxation dispersion profiles for the WT E:THF:NADPH complex at 300 K, pH 7.6.

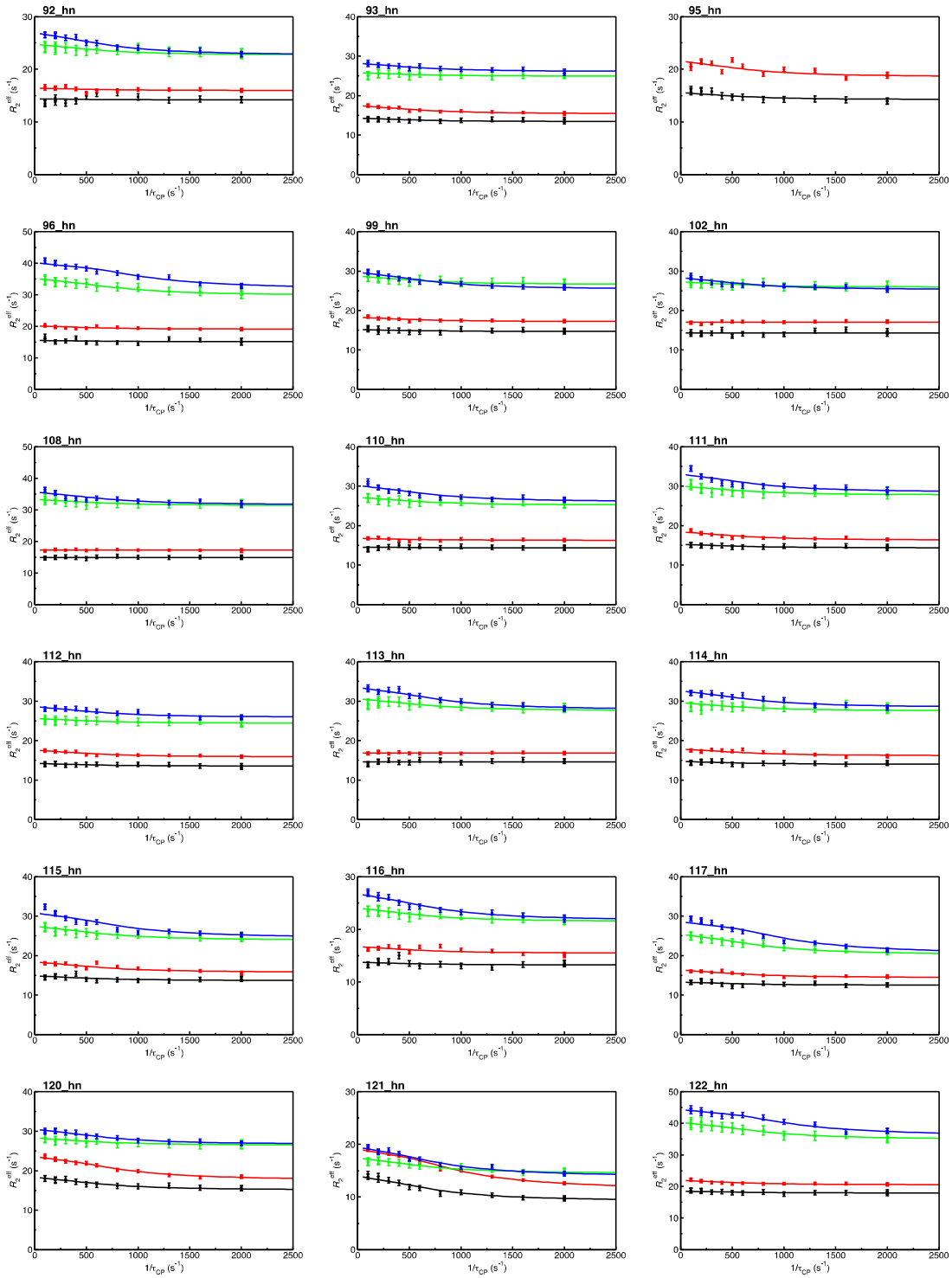

Figure S2 (Continued). R_2 relaxation dispersion profiles for the WT E:THF:NADPH complex at 300 K, pH 7.6.

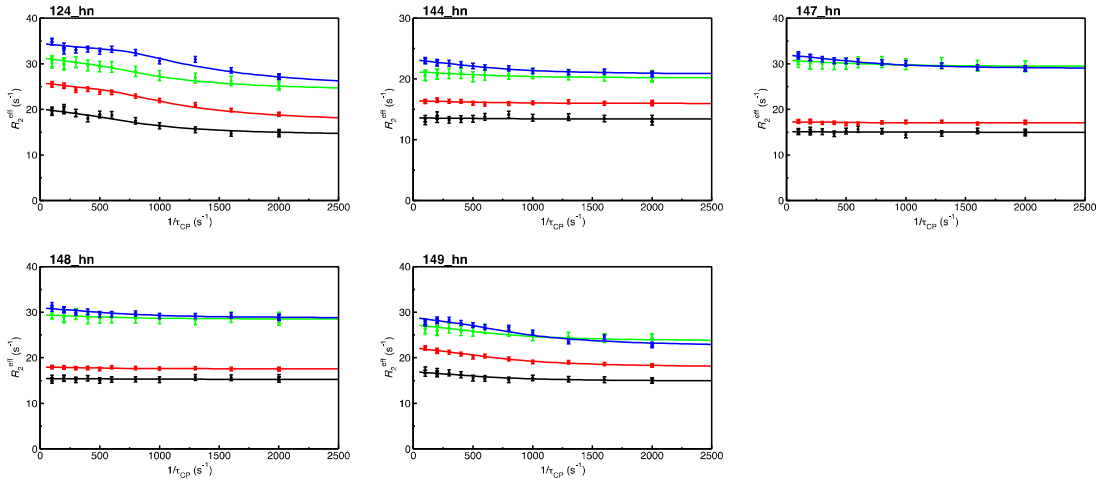

Figure S2 (Continued). R_2 relaxation dispersion profiles for the WT E:THF:NADPH complex at 300 K, pH 7.6.

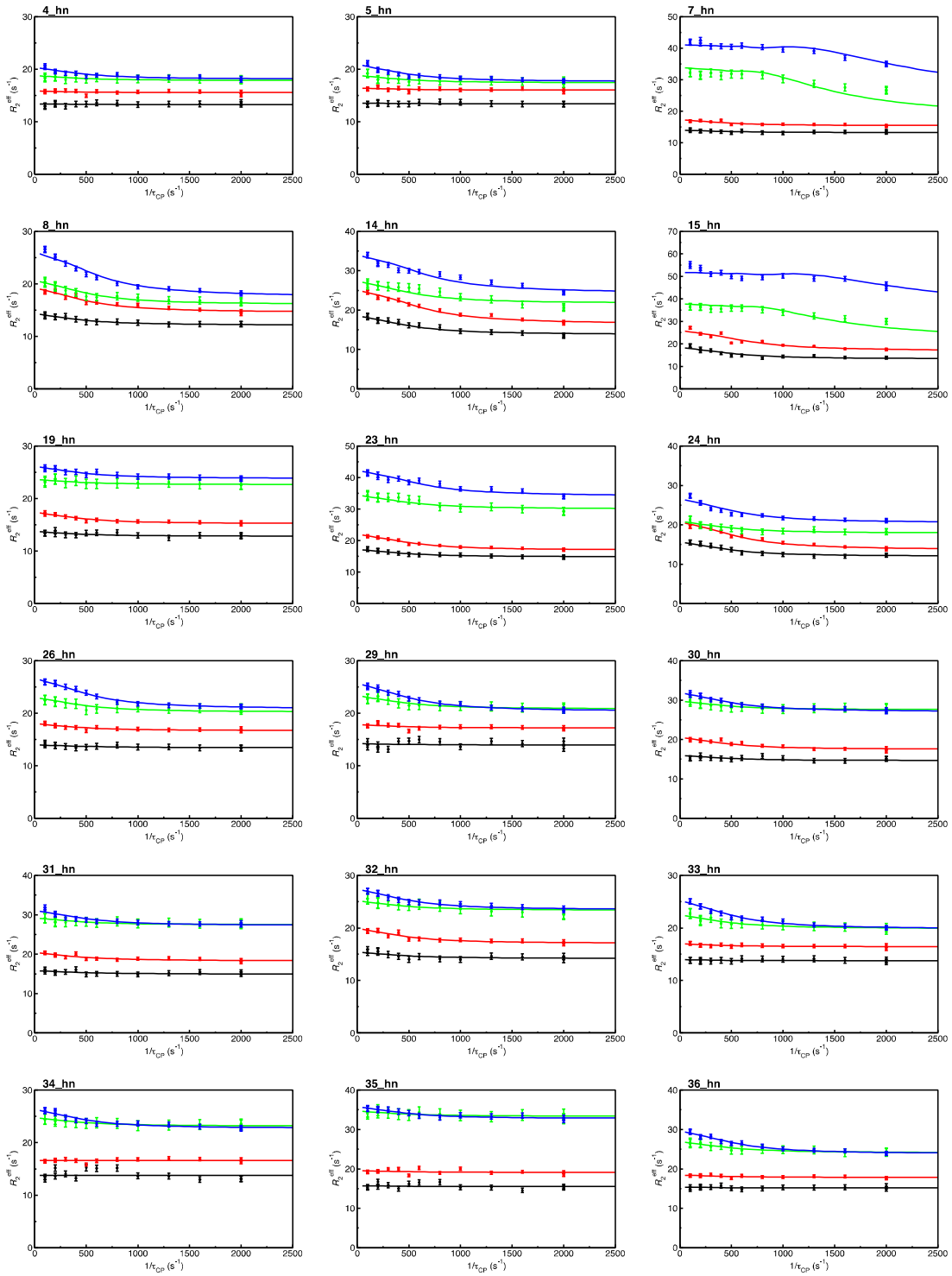

Figure S3. R_2 relaxation dispersion profiles for the WT E:THF:NADP$^+$ complex at 300 K, pH 7.6. Black and red, amide ^{15}N dispersion data at 11.7 and 18.8 T, respectively. Green and blue, amide ^{1}H dispersion data at 11.7 (500 MHz) and 18.8 T (800 MHz), respectively. Solid lines indicate the best fit of the data to a global two-site exchange model.

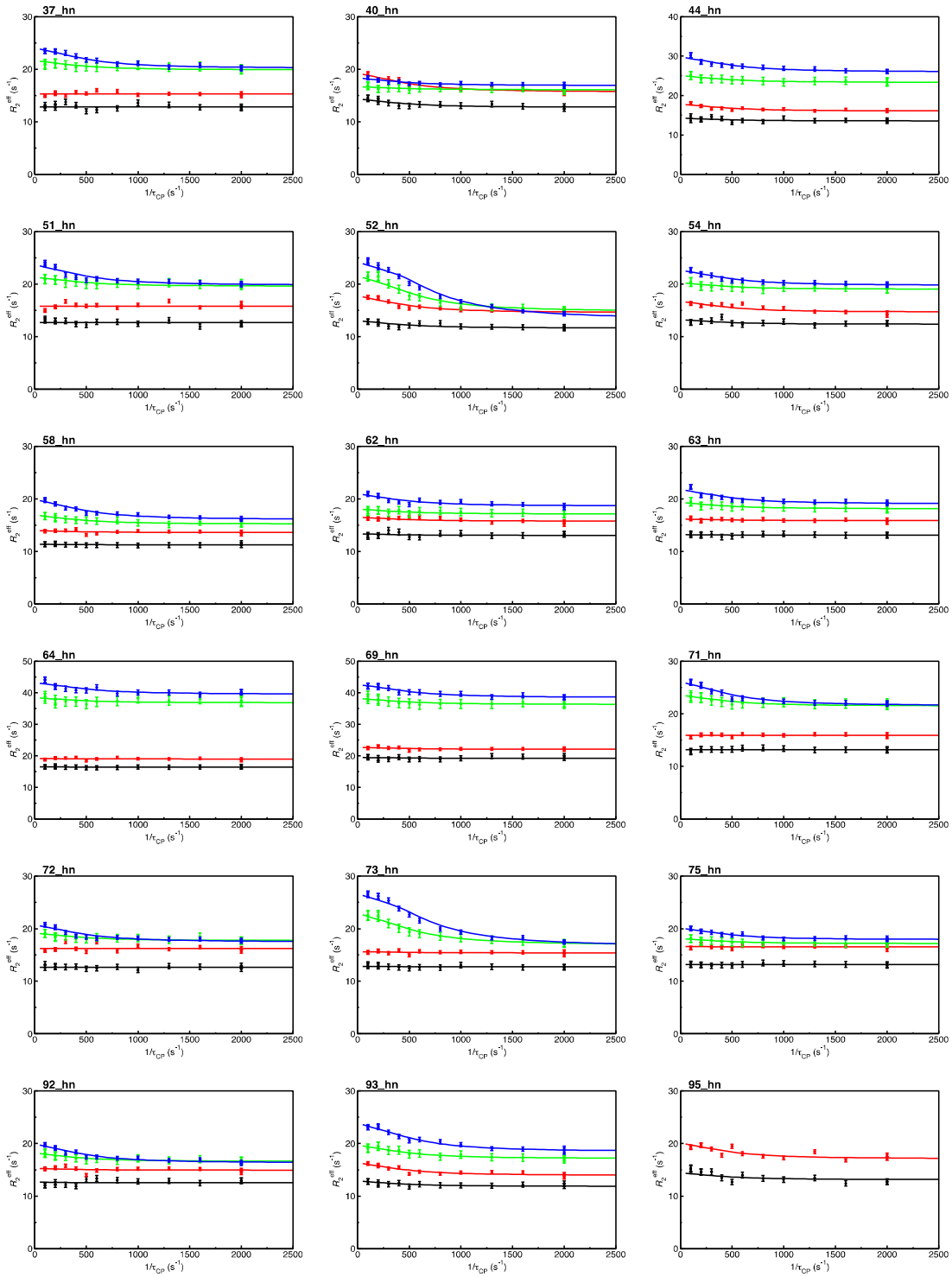

Figure S3 (Continued). R_2 **relaxation** dispersion profiles for the WT E:THF:NADP+ complex at 300 K, pH 7.6.

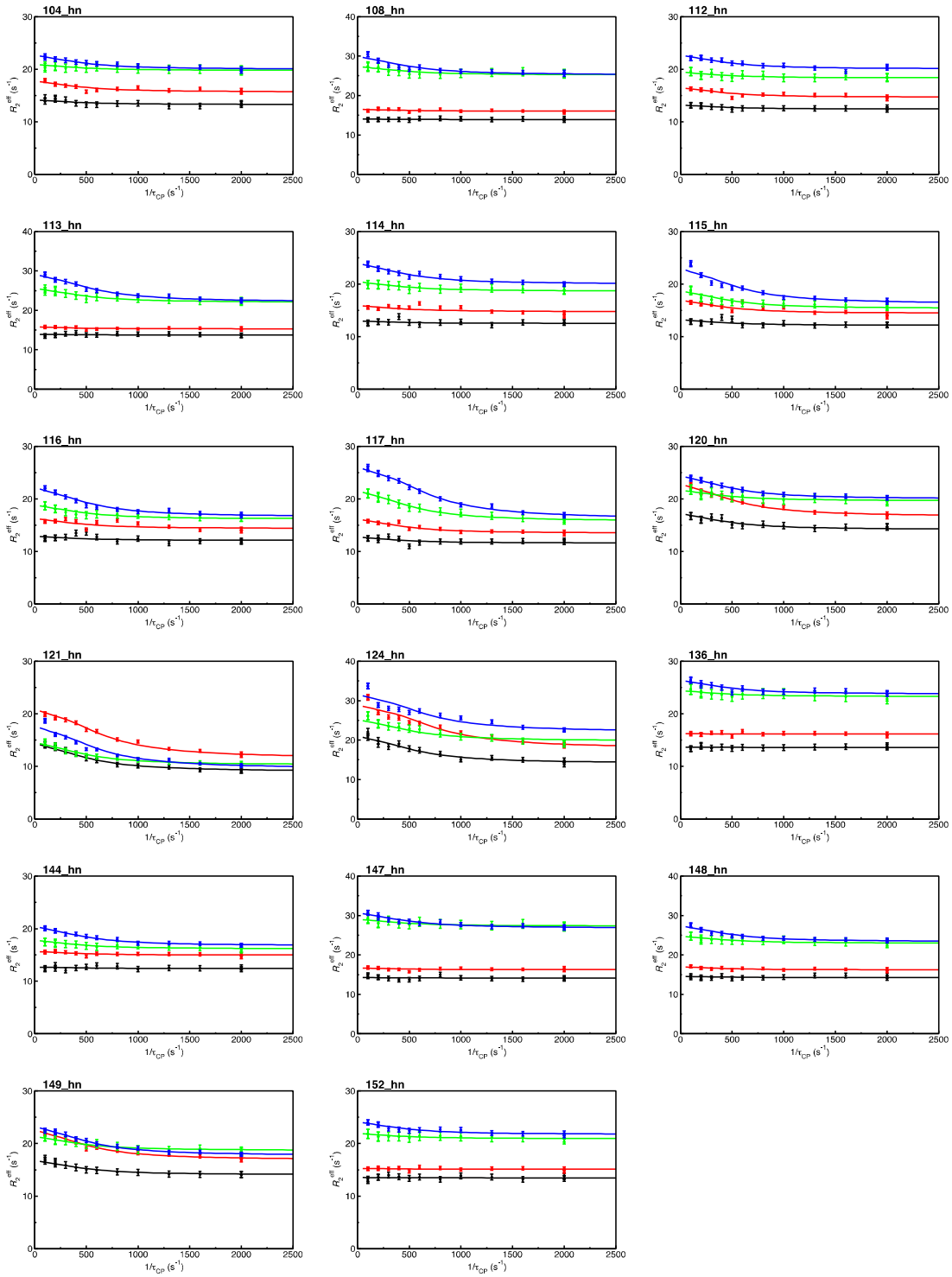

Figure S3 (Continued). R_2 relaxation dispersion profiles for the WT E:THF:NADP$^+$ complex at 300 K, pH 7.6.

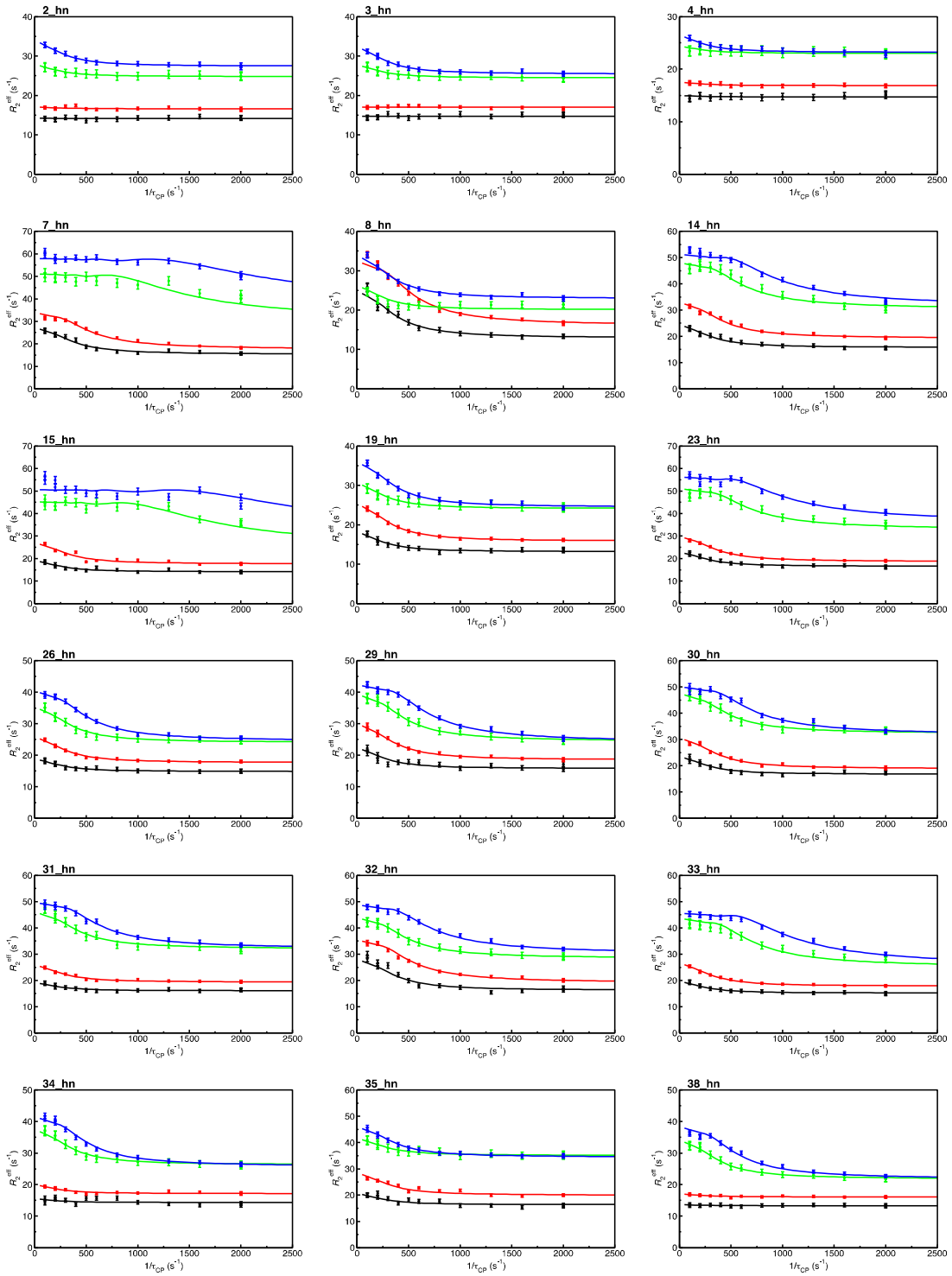

Figure S4. R_2 relaxation dispersion profiles for the L28F E:THF:NADPH complex at 300 K, pH 7.6. Black and red, amide ^{15}N dispersion data at 11.7 and 18.8 T, respectively. Green and blue, amide ^{1}H dispersion data at 11.7 (500 MHz) and 18.8 T (800 MHz), respectively. Solid lines indicate the best fit of the data to a global two-site exchange model.

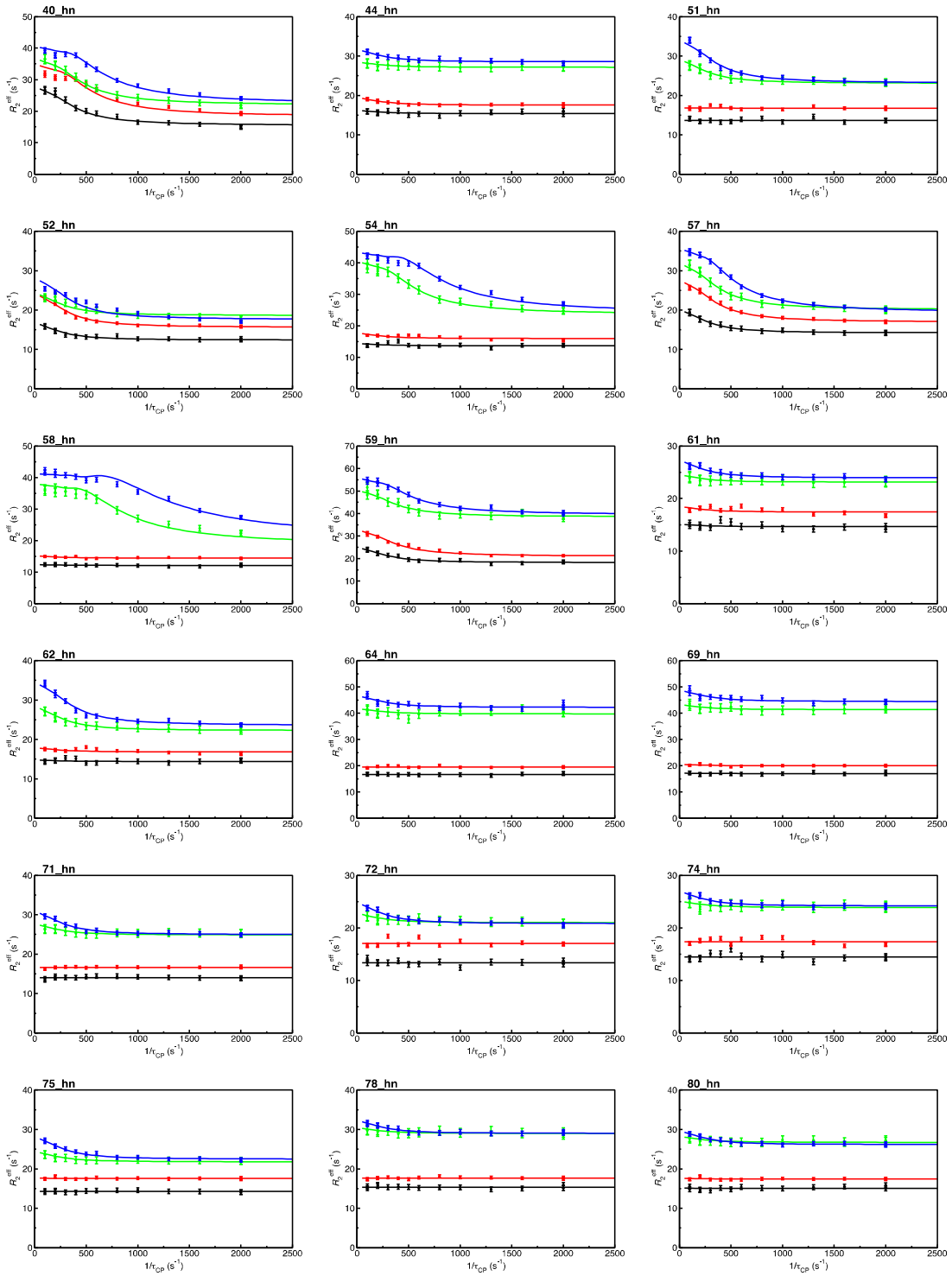

Figure S4 (Continued). R_2 relaxation dispersion profiles for the L28F E:THF:NADPH complex at 300 K, pH 7.6.

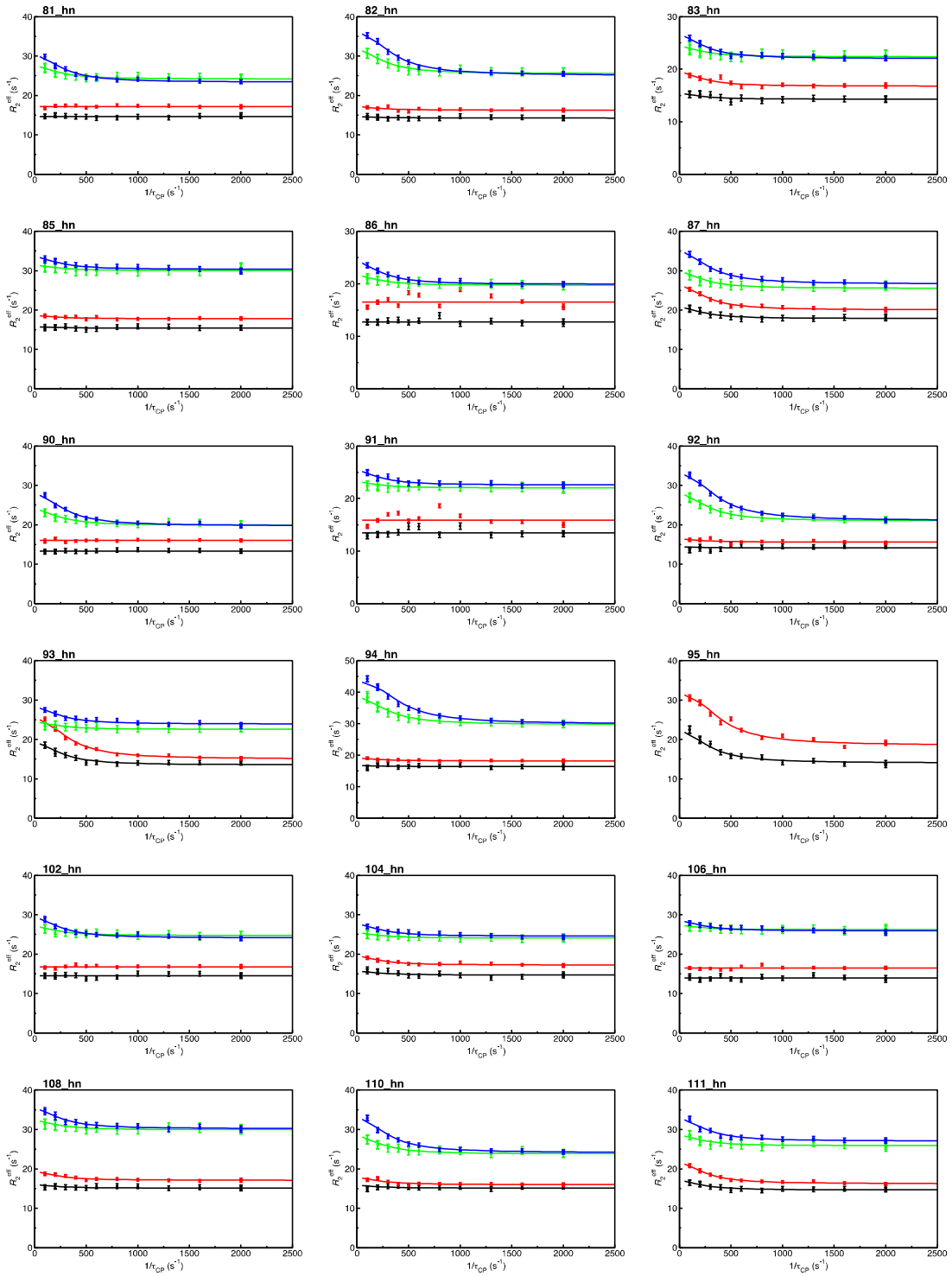

Figure S4 (Continued). R_2 relaxation dispersion profiles for the L28F E:THF:NADPH complex at 300 K, pH 7.6.

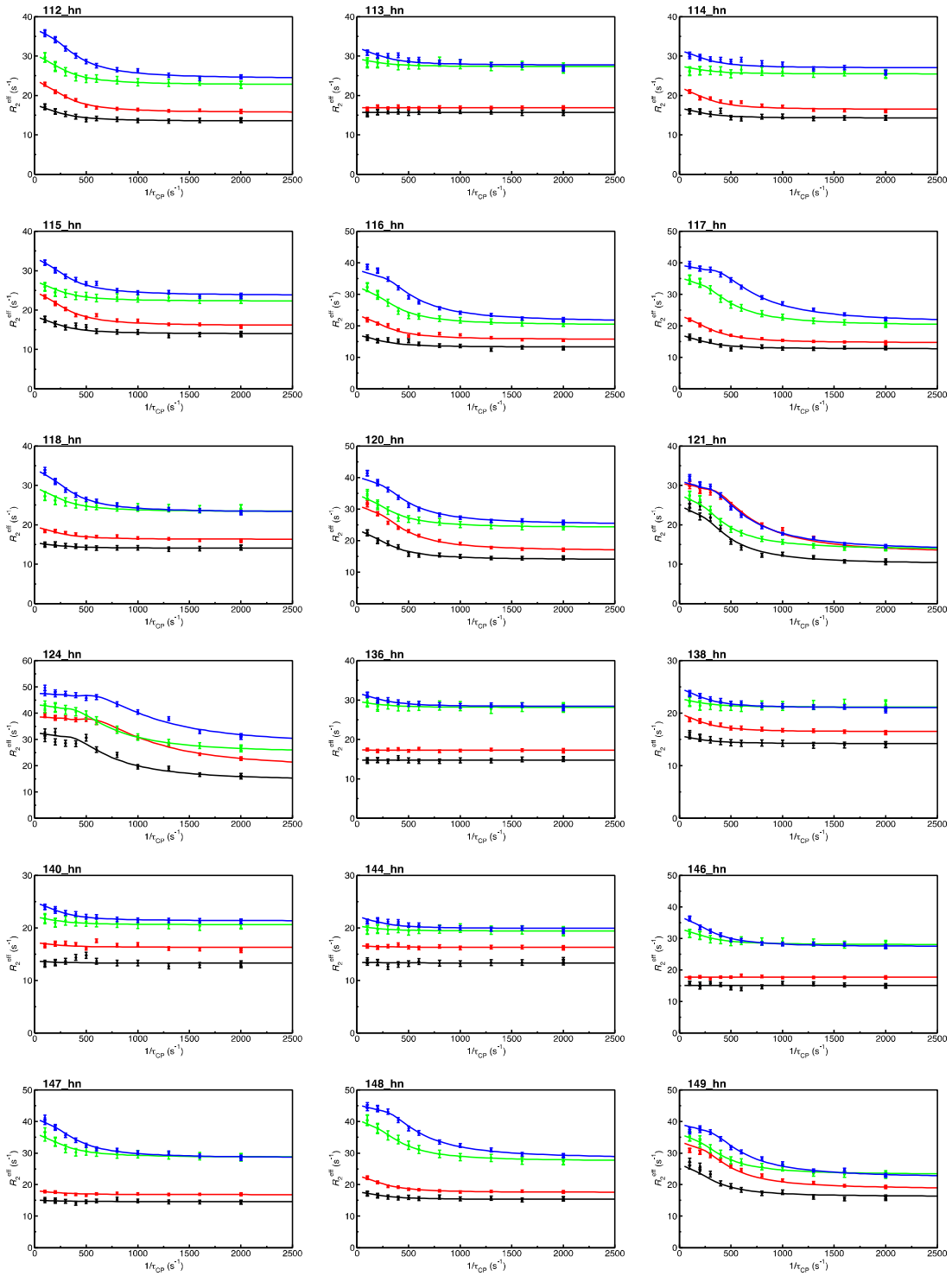

Figure S4 (Continued). R_2 relaxation dispersion profiles for the L28F E:THF:NADPH complex at 300 K, pH 7.6.

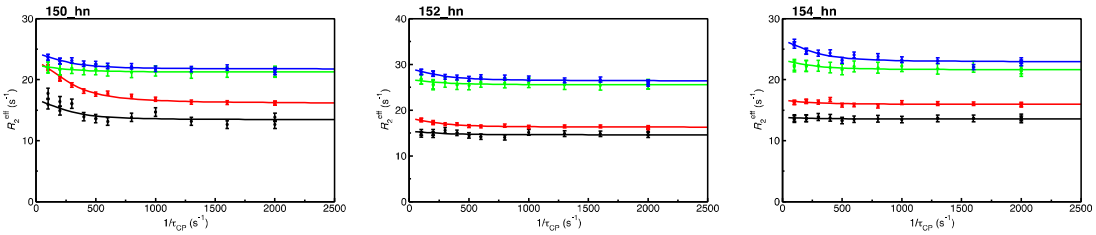

Figure S4 (Continued). R_2 relaxation dispersion profiles for the L28F E:THF:NADPH complex at 300 K, pH 7.6.

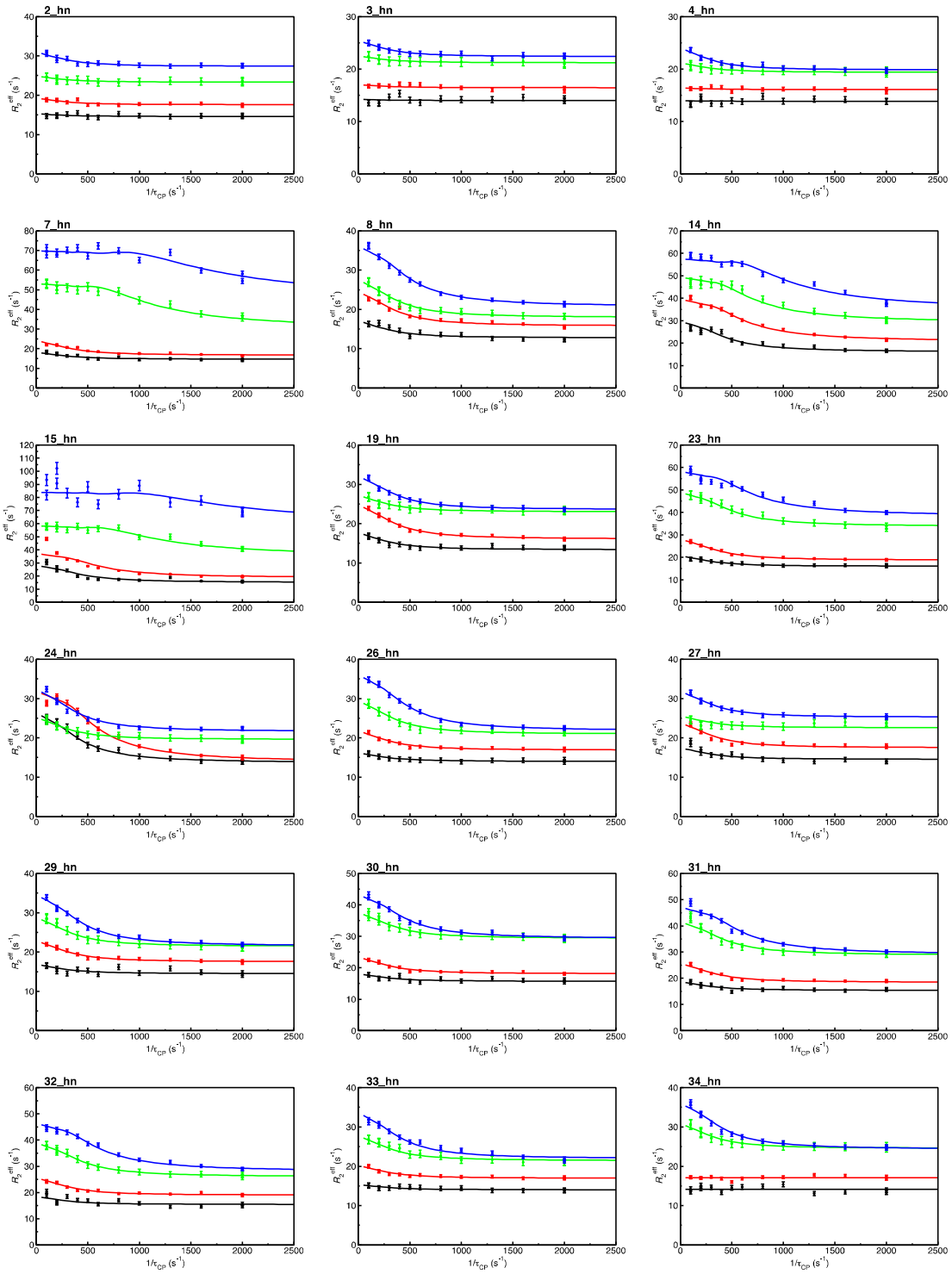

Figure S5. R_2 relaxation dispersion profiles for the L28F E:THF:NADP$^+$ complex at 300 K, pH 7.6. Black and red, amide ^{15}N dispersion data at 11.7 and 18.8 T, respectively. Green and blue, amide ^{1}H dispersion data at 11.7 (500 MHz) and 18.8 T (800 MHz), respectively. Solid lines indicate the best fit of the data to a global two-site exchange model.

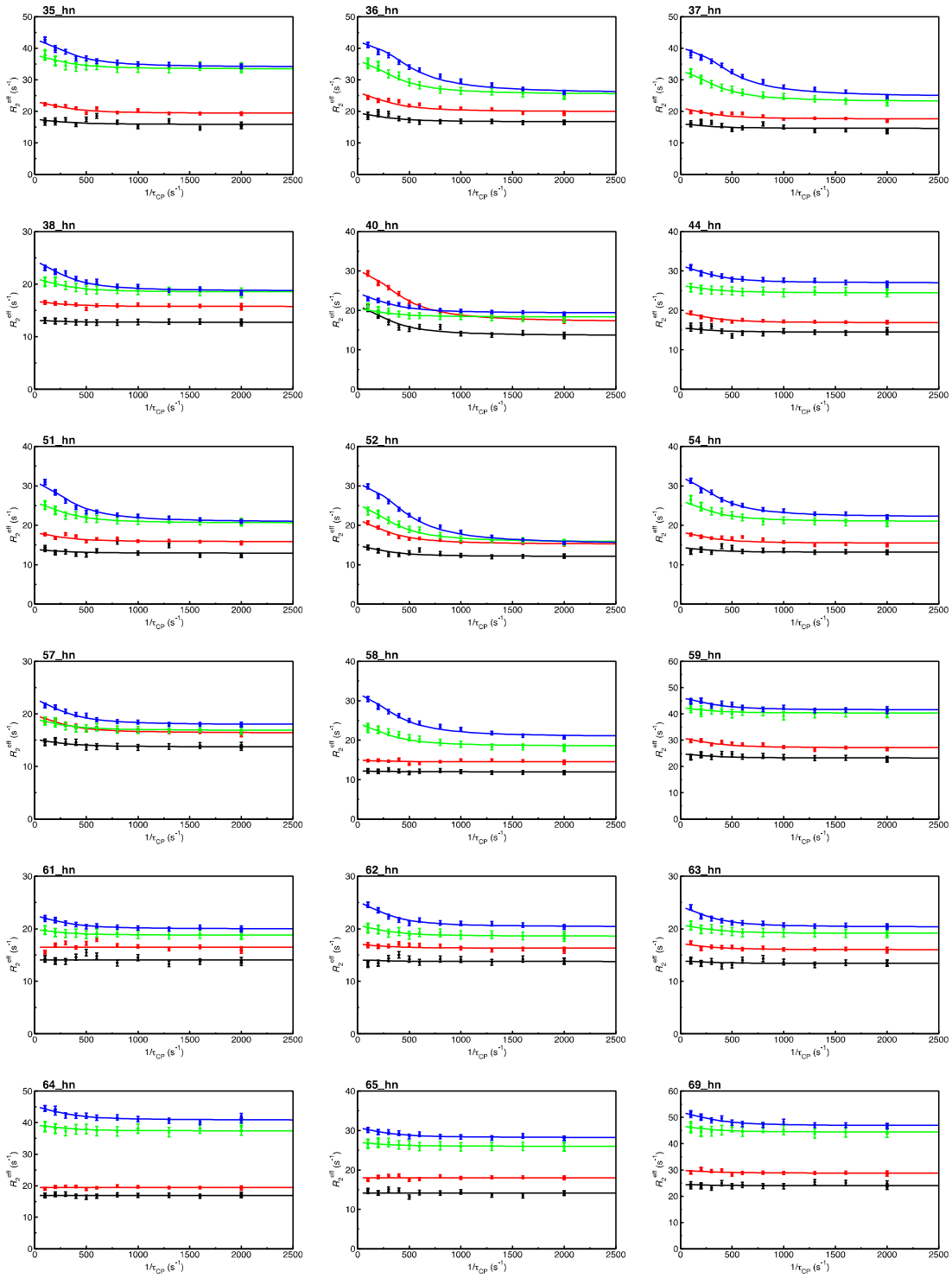

Figure S5 (Continued). R_2 relaxation dispersion profiles for the L28F E:THF:NADP$^+$ complex at 300 K, pH 7.6.

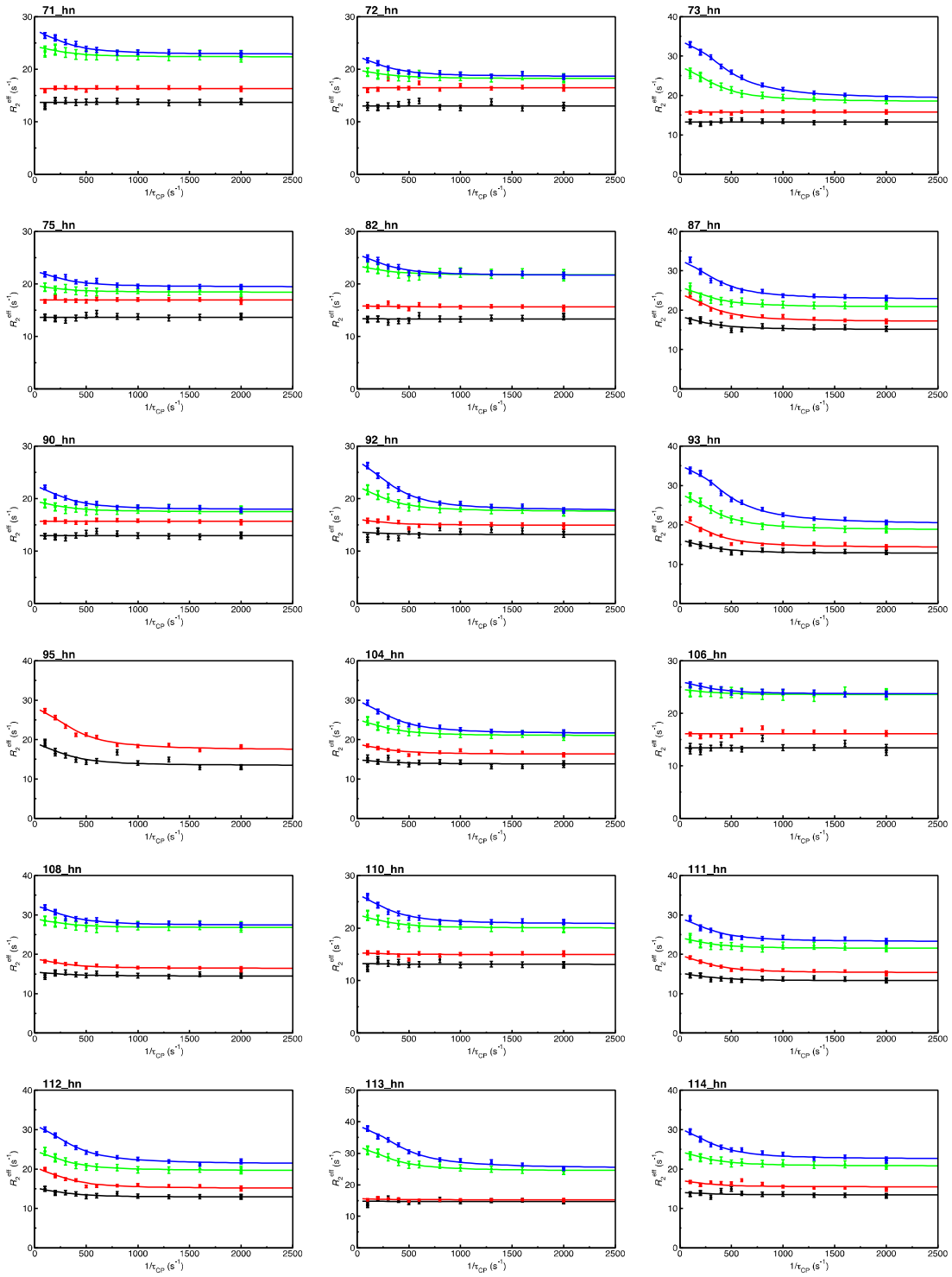

Figure S5 (Continued). R_2 relaxation dispersion profiles for the L28F E:THF:NADP$^+$ complex at 300 K, pH 7.6.

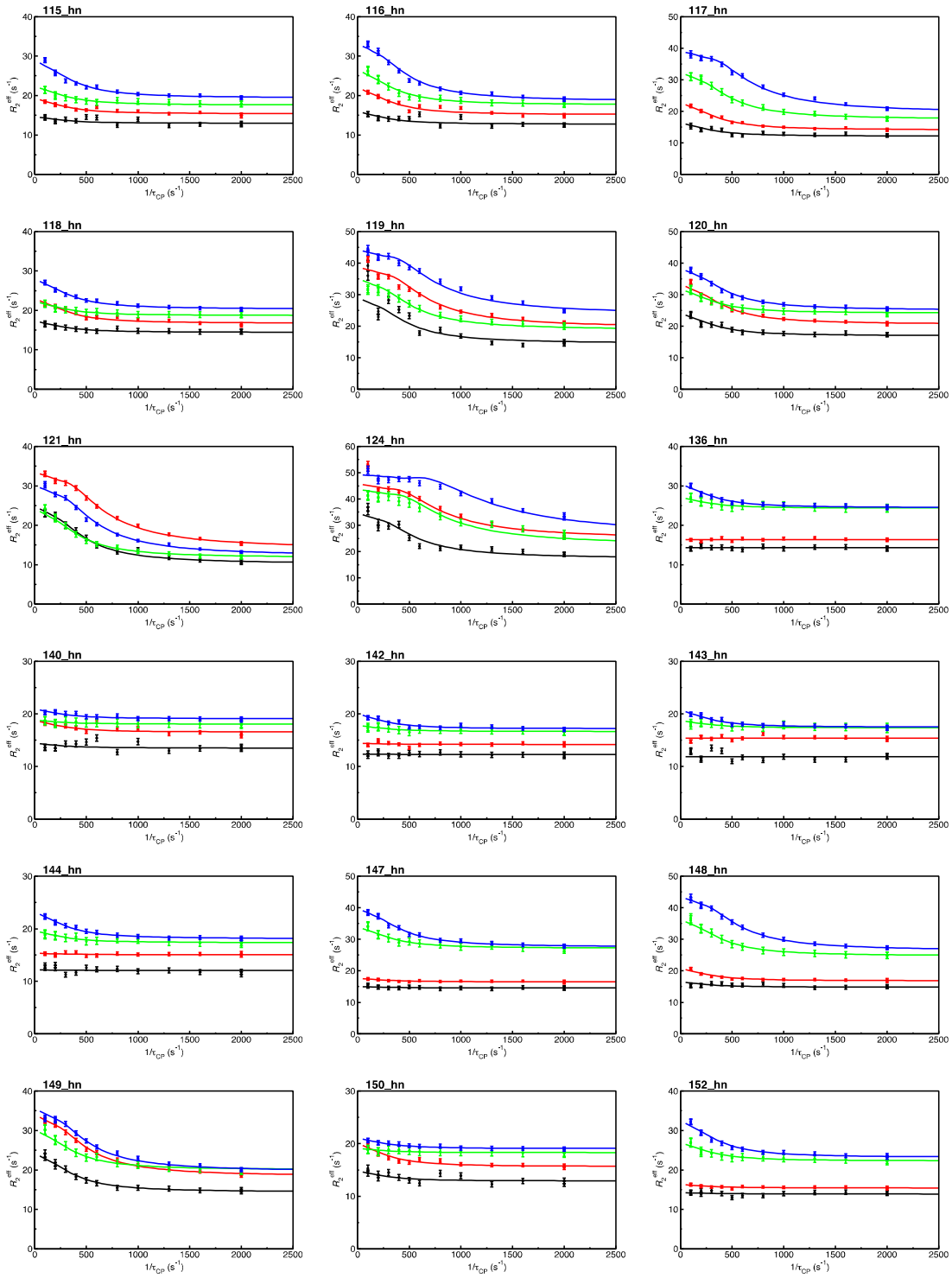

Figure S5 (Continued). R_2 relaxation dispersion profiles for the L28F E:THF:NADP$^+$ complex at 300 K, pH 7.6.

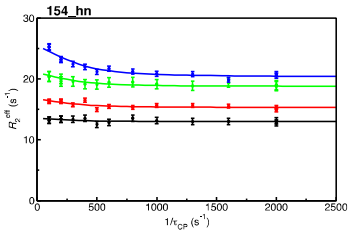

Figure S5 (Continued). R_2 relaxation dispersion profiles for the L28F E:THF:NADP+ complex at 300 K, pH 7.6.

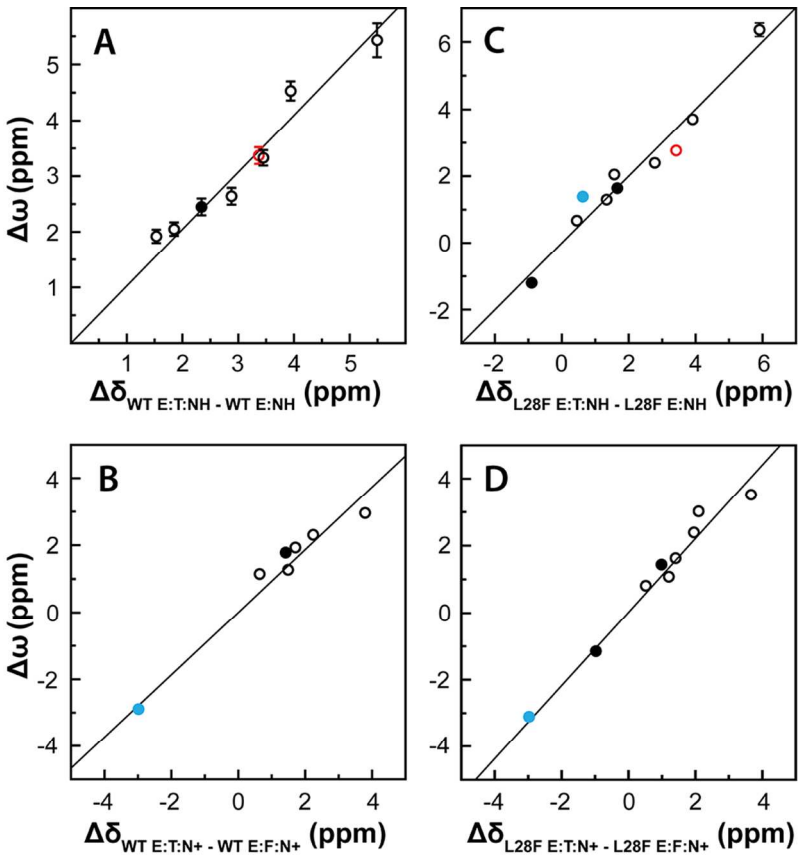

Figure S6. Correlations between the dynamic chemical shift differences $\Delta\omega_N$ and equilibrium chemical shift differences ($\Delta\delta_N$) for a subset of residues that have been identified as markers for the occluded-to-closed transition (N23, L24, I94, G95, I115, D116, E118, G121, H124, and H149; black) and markers for binding of the nicotinamide ring in the active site (A7; red, and G15; cyan). The equilibrium shift differences ($\Delta\delta_N$) are the differences in chemical shift between the occluded E:THF:NADPH or E:THF:NADP$^+$ complexes and the closed E:NADPH or E:FOL:NADP$^+$ complexes, respectively. Filled symbols represent residues for which the sign of $\Delta\omega_N$ could be determined from the HMQC-HSQC experiment; otherwise the absolute value of $\Delta\omega_N$ is plotted. Lines of best fit obtained by linear regression through the origin are shown for A. the WT E:THF:NADPH complex (slope = 1.02 ± 0.02, R^2 = 0.95), B. the WT E:THF:NADP$^+$ complex (slope = 0.93 ± 0.04, R^2 = 0.95), C. the L28F E:THF:NADPH complex (slope = 1.00 ± 0.02, R^2 = 0.95), D. the L28F E:THF:NADP$^+$ complex (slope = 1.10 ± 0.03, R^2 = 0.97).

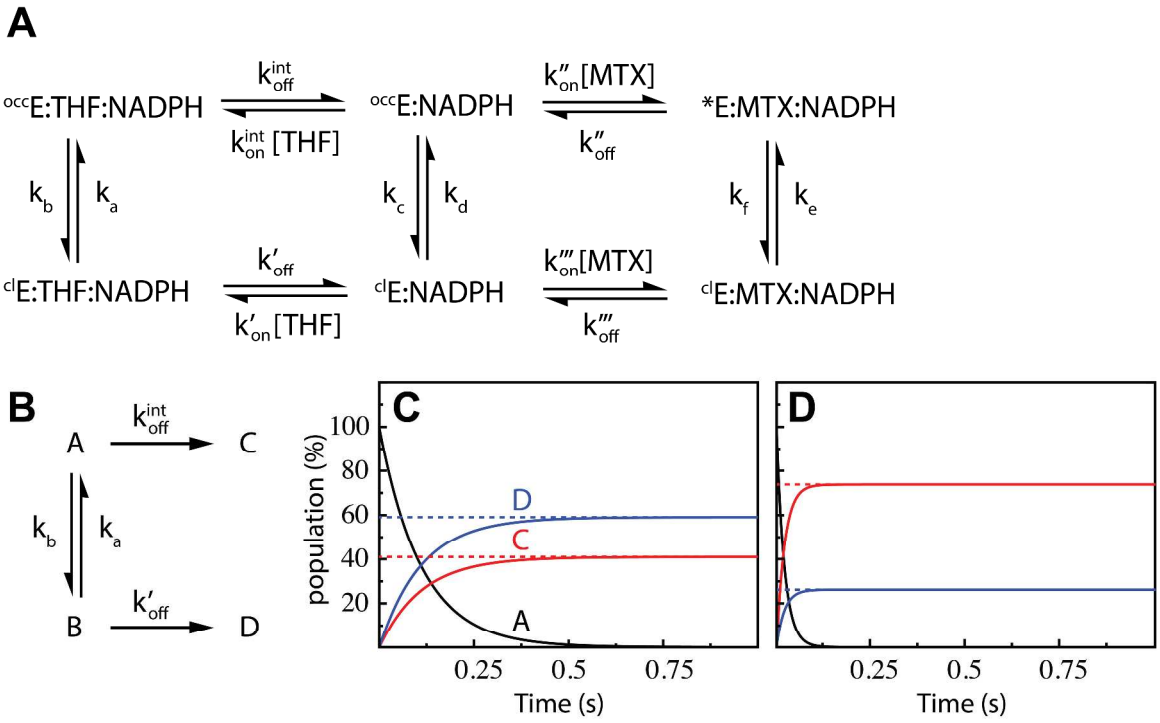

Figure S7. A) Expanded kinetic scheme for stopped-flow competition experiments; each enzyme species exchanges between a major and a minor conformational substate. The asterisk denotes the minor occluded conformational substate for the E:MTX:NADPH complex. B) Simplified kinetic scheme for stopped-flow competition experiments under the condition where a large excess of MTX is used. Simulations of this kinetic scheme were performed with Tenua (freely available from bilite.com/tenua) using the kinetic rates determined in the present work. The presence of a small population of state B present at the start of the competition experiment does not significantly alter the observed rate constant. C) Simulated progress curves (A: black, C: red, D: blue) for the WT E:THF:NADPH complex confirm the observed dissociation rate of 9 s^{-1} and the 41%/59% partitioning ratio for the intrinsic and allosteric pathway respectively. D) Simulated progress curves (A: black, C: red, D: blue) for the L28F E:THF:NADPH complex confirm the observed dissociation rate of 48 s^{-1} and the 75%/25% partitioning ratio for the intrinsic and allosteric pathway respectively. The progress curve for B is not displayed in the figure since its population remains well below 5%.

Table S1. Data collection and refinement statistics

	WT ecDHFR:THF:NADP+	L28F ecDHFR:THF:NADP+
Data collection		
Beamline	SSRL BL11-1	SSRL BL11-1
Wavelength (Å)	0.97945	0.97945
Space group	$P2_12_12_1$	$P2_12_12_1$
Cell dimensions		
a, *b*, *c* (Å)	34.13, 58.20, 75.21	34.54, 58.25, 79.38
α, β, γ (°)	90.00, 90.00, 90.00	90.00, 90.00, 90.00
Resolution (Å)	46.03-1.50 (1.53-1.50)*	46.96-1.20 (1.22-1.20)
R_{sym} (%)	7.7 (95.9)	4.6 (100)
R_{meas} (%)	7.9 (100)	4.8 (100)
R_{pim} (%)	2.3 (38.3)	1.5 (36.6)
$CC_{1/2}$ (%)	90.2 (50.3)	93.5 (76.3)
I / σI	33.1 (1.9)	43.8 (2.0)
Total reflections	278,485	616,803
Unique reflections	24,646 (1,160)	50,682 (2,468)
Completeness (%)	99.6 (96.8)	99.2 (98.6)
Redundancy	11.3 (6.8)	12.2 (12.2)
Refinement		
Resolution (Å)	46.03-1.50	46.96-1.20
Reflections (work/free)	23,341/1,253	48,045/2,574
R_{work} / R_{free} (%)	17.1/23.8	15.5/19.6
No. atoms		
Protein	1304	1397
Ligands	80	128
Water	134	239
B-factors		
Protein	30.1	20.4
Ligands	36.4	24.4
Water	35.7	33.0
R.m.s. deviations		
Bond lengths (Å)	0.011	0.009
Bond angles (°)	1.34	1.32
Ramachandran plot distribution from MolProbity		
Favored (%)	96.95	98.31
Allowed (%)	3.05	1.13
Outliers (%)	0.00	0.56

*Values in parentheses are for highest-resolution shell.

Table S2. Fitted values of R_{ex} (at 18.8 T) and $|\Delta\omega_N|$ for amide ^{15}N probes in the WT E:THF:NADPH complex. Residues with R_{ex} smaller than 2 s^{-1} are omitted. The X^2 per degree of freedom (DoF) is calculated from the combined fit of ^{15}N and ^{1}H amide dispersion data to the global k_{ex} and p_b, except for Gly95 where only ^{15}N data are available. The equilibrium shift difference $\Delta\delta_N$ is calculated as the difference in ^{15}N chemical shift between the WT E:THF:NADPH and WT E:NADPH complexes. The ^{15}N and ^{1}H resonances of Ile14 have not been assigned for the WT E:NADPH complex, hence the $\Delta\delta_N$ is unavailable for that residue.

Residue	R_{ex} (s^{-1})	$\|\Delta\omega_N\|$ (ppm)	error (ppm)	sign	X^2/DoF	$\Delta\delta_N$ (ppm)
Ala7	5.65	3.37	0.15	ND	0.85	-3.37
Leu8	6.19	3.66	0.20	ND	0.66	1.65
Ile14	4.05	2.59	0.13	ND	0.41	N/A
Asn23	3.74	2.45	0.15	+	0.19	2.34
Leu24	5.58	3.33	0.14	ND	0.20	-3.45
Asp27	2.32	1.80	0.15	ND	0.26	2.51
Trp30	3.94	2.54	0.14	ND	0.43	1.95
Lys32	4.56	2.83	0.16	ND	0.49	2.17
Arg33	2.40	1.84	0.15	ND	0.36	0.86
Leu36	5.98	3.54	0.19	ND	0.33	-2.35
Asn37	4.67	2.88	0.13	ND	0.94	-2.11
Val40	5.10	3.09	0.17	ND	0.31	2.68
Asn59	2.49	1.88	0.20	ND	0.35	1.32
Val93	2.01	1.65	0.13	ND	0.28	-1.60
Gly95	2.87	2.05	0.12	ND	1.95	1.85
Tyr111	2.00	1.65	0.14	ND	0.79	-0.47
Ile115	2.58	1.92	0.12	ND	1.26	1.53
Glu120	5.83	3.47	0.18	ND	0.18	1.84
Gly121	7.59	4.53	0.17	ND	0.64	3.94
His124	8.69	5.43	0.30	ND	0.58	-5.49
His149	4.15	2.64	0.15	ND	0.52	2.88

Table S3. Fitted values of R_{ex} (at 18.8 T, 800 MHz) and $|\Delta\omega_H|$ for amide ^1H probes in the WT E:THF:NADPH complex. Residues with R_{ex} smaller than 2 s^{-1} are omitted. The X^2 per degree of freedom (DoF) is calculated from the combined fit of ^{15}N and ^1H amide dispersion data to the global k_{ex} and p_b. The equilibrium shift difference $\Delta\delta_H$ is calculated as the difference in amide ^1H chemical shift between the WT E:THF:NADPH and WT E:NADPH complexes. The ^{15}N and ^1H resonances of Ile14 and Lys38 have not been assigned for the WT E:NADPH complex, hence $\Delta\delta_H$ is unavailable for those residues.

Residue	R_{ex} (s^{-1})	$\|\Delta\omega_H\|$ (ppm)	error (ppm)	X^2/DoF	$\Delta\delta_H$ (ppm)
Ile5	3.48	0.24	0.02	0.20	0.12
Ala7	12.28	1.56	0.09	0.85	-1.95
Leu8	5.00	0.31	0.03	0.66	-0.05
Ile14	9.00	0.58	0.06	0.41	N/A
Gly15	12.17	1.45	0.11	1.81	1.57
Met16	5.23	0.32	0.02	0.60	0.04
Ala19	2.78	0.20	0.02	0.36	0.05
Asn23	8.57	0.54	0.10	0.19	0.69
Ala26	4.60	0.29	0.02	0.26	-0.34
Asp27	2.64	0.20	0.02	0.26	-0.41
Ala29	5.23	0.32	0.02	0.57	0.36
Trp30	4.92	0.30	0.03	0.43	0.33
Phe31	2.02	0.17	0.03	0.23	0.14
Lys32	2.38	0.19	0.02	0.49	0.41
Arg33	7.74	0.47	0.03	0.36	0.49
Asn34	4.14	0.27	0.02	0.85	0.20
Thr35	2.32	0.18	0.03	1.03	0.07
Leu36	7.76	0.47	0.04	0.33	0.53
Asn37	5.48	0.33	0.03	0.94	-0.47
Lys38	3.98	0.26	0.02	0.34	N/A
Val40	5.09	0.31	0.02	0.31	0.20
Arg44	2.04	0.17	0.02	0.35	-0.03
Gly51	3.25	0.23	0.02	1.15	-0.08
Leu54	6.08	0.36	0.03	0.32	-0.43
Arg57	4.03	0.26	0.02	0.20	0.03
Lys58	8.15	0.50	0.04	0.25	-0.54
Asn59	2.62	0.20	0.04	0.35	0.10
Leu62	2.17	0.17	0.02	0.37	0.06
Ser64	4.15	0.27	0.04	0.72	-0.06
Asp69	3.29	0.23	0.04	0.42	-0.05
Arg71	3.45	0.23	0.02	0.49	-0.07
Val72	2.88	0.21	0.02	1.14	-0.07
Val75	2.46	0.19	0.02	0.20	0.02
Ile82	2.39	0.19	0.02	0.20	0.06
Glu90	2.11	0.17	0.02	0.24	0.00
Met92	4.12	0.27	0.02	0.70	0.05
Val93	2.01	0.17	0.02	0.28	-0.06
Gly96	8.29	0.51	0.07	0.60	0.46
Val99	4.18	0.27	0.02	0.25	-0.21
Gln102	2.9	0.21	0.02	0.55	0.00

Gln108	3.93	0.26	0.02	0.39	0.00
Leu110	4.00	0.26	0.02	0.50	0.04
Tyr111	4.44	0.28	0.02	0.79	-0.04
Leu112	2.62	0.20	0.02	0.25	0.03
Thr113	5.54	0.34	0.02	0.34	-0.06
His114	4.04	0.26	0.02	0.62	-0.07
Ile115	6.19	0.37	0.02	1.26	0.07
Asp116	4.90	0.30	0.02	1.00	-0.27
Ala117	8.08	0.50	0.04	0.75	0.34
Glu120	3.72	0.25	0.02	0.18	0.14
Gly121	5.43	0.33	0.01	0.64	-0.36
Asp122	8.35	0.52	0.06	0.24	-0.53
His124	9.90	0.69	0.08	0.58	-0.89
Asp144	2.28	0.18	0.02	0.22	0.00
Asn147	2.92	0.21	0.02	0.20	0.07
Ser148	2.16	0.17	0.02	0.15	-0.19
His149	6.33	0.38	0.02	0.52	0.23

Table S4. Fitted values of R_{ex} (at 18.8 T) and $|\Delta\omega_N|$ for amide ^{15}N probes in the WT E:THF:NADP$^+$ complex. Residues with R_{ex} smaller than 2 s^{-1} are omitted. The X^2 per degree of freedom (DoF) is calculated from the combined fit of ^{15}N and ^1H amide dispersion data to the global k_{ex} and p_b, except for Gly95 where only ^{15}N data are available. The equilibrium shift difference $\Delta\delta_N$ is calculated as the difference in ^{15}N chemical shift between the WT E:THF:NADP$^+$ and WT E:FOL:NADP$^+$ complexes. The ^{15}N and ^1H resonances of His124 have not been assigned for the WT E:FOL:NADP$^+$ complex, hence $\Delta\delta_N$ is not available for that residue.

Residue	R_{ex} (s^{-1})	$\lvert\Delta\omega_N\rvert$ (ppm)	error (ppm)	sign	X^2/DoF	$\Delta\delta_N$ (ppm)
Leu8	4.41	1.69	0.07	ND	0.79	0.46
Ile14	8.32	2.75	0.07	ND	1.22	3.09
Gly15	8.78	2.89	0.08	-	2.90	-2.98
Ala19	2.01	1.06	0.07	ND	0.23	0.21
Asn23	4.76	1.78	0.08	+	0.45	1.42
Leu24	6.79	2.31	0.07	ND	0.91	-2.24
Trp30	2.87	1.30	0.09	ND	0.49	0.61
Lys32	2.65	1.24	0.06	ND	0.43	-0.37
Val40	3.41	1.44	0.08	ND	0.45	1.24
Arg52	2.99	1.33	0.05	ND	0.79	0.23
Val93	2.23	1.12	0.07	ND	0.63	-0.87
Gly95	2.78	1.27	0.08	ND	2.06	1.49
Ile115	2.33	1.15	0.07	ND	1.68	0.64
Ala117	2.50	1.20	0.06	+	0.57	0.75
Glu120	5.84	2.06	0.08	ND	0.29	1.94
Gly121	8.98	2.96	0.06	ND	1.67	3.79
His124	10.72	3.59	0.10	+	2.99	N/A
His149	5.35	1.93	0.07	ND	0.27	1.71

Table S5. Fitted values of R_{ex} (at 18.8 T, 800 MHz) and $|\Delta\omega_H|$ for amide ^1H probes in the WT E:THF:NADPH$^+$ complex. Residues with R_{ex} smaller than 2 s^{-1} are omitted. The X^2 per degree of freedom (DoF) is calculated from the combined fit of ^{15}N and ^1H amide dispersion curves to the global k_{ex} and p_b. The equilibrium shift difference $\Delta\delta_H$ is calculated as the difference in amide proton chemical shift between the WT E:THF:NADP$^+$ and WT E:FOL:NADP$^+$ complexes. The ^{15}N and ^1H resonances of Ala7 and His124 have not been assigned for the WT E:FOL:NADP$^+$ complex, hence $\Delta\delta_H$ is unavailable for those residues.

Residue	R_{ex} (s^{-1})	$\lvert\Delta\omega_H\rvert$ (ppm)	error (ppm)	X^2/DoF	$\Delta\delta_H$ (ppm)
Leu4	2.06	0.11	0.01	0.46	-0.08
Ile5	3.05	0.14	0.01	0.46	-0.02
Ala7	16.98	1.36	0.06	1.24	N/A
Leu8	8.13	0.27	0.01	0.79	-0.15
Ile14	9.32	0.31	0.01	1.22	-0.78
Gly15	17.00	1.37	0.07	2.90	1.36
Ala19	2.15	0.11	0.01	0.23	-0.02
Asn23	7.81	0.26	0.02	0.45	0.49
Leu24	5.78	0.21	0.01	0.91	-0.13
Ala26	5.50	0.20	0.01	0.24	-0.18
Ala29	5.03	0.19	0.01	0.72	0.21
Trp30	4.52	0.17	0.01	0.49	0.19
Phe31	3.63	0.15	0.01	0.51	0.38
Lys32	3.70	0.15	0.01	0.43	0.24
Arg33	5.12	0.19	0.01	0.28	0.28
Asn34	3.37	0.14	0.01	0.93	0.16
Thr35	2.83	0.13	0.01	0.87	0.10
Leu36	5.52	0.20	0.01	0.26	0.21
Asn37	3.65	0.15	0.01	0.67	0.00
Arg44	3.59	0.15	0.01	0.52	-0.02
Gly51	3.67	0.15	0.01	1.25	0.15
Arg52	10.67	0.36	0.01	0.79	0.11
Leu54	2.73	0.13	0.01	0.73	-0.06
Lys58	3.60	0.15	0.01	0.43	0.01
Leu62	2.15	0.11	0.01	0.68	-0.08
Ser63	2.59	0.12	0.01	0.41	-0.05
Ser64	3.48	0.15	0.02	0.46	-0.02
Asp69	3.94	0.16	0.01	0.27	0.04
Arg71	4.30	0.17	0.01	0.37	0.01
Val72	3.05	0.14	0.01	1.20	-0.01
Thr73	9.82	0.33	0.01	0.62	-0.04
Val75	2.09	0.11	0.01	0.33	-0.01
Met92	3.38	0.14	0.01	1.00	0.09
Val93	5.11	0.19	0.01	0.63	-0.13
Leu104	2.47	0.12	0.01	0.48	0.14
Gln108	4.41	0.17	0.01	0.51	0.01
Leu112	2.43	0.12	0.01	0.51	0.12
Thr113	6.68	0.23	0.01	0.31	-0.18
His114	3.69	0.15	0.01	1.08	0.04
Ile115	6.36	0.22	0.01	1.68	0.01

Asp116	5.24	0.19	0.01	1.46	-0.22
Ala117	9.58	0.32	0.01	0.57	0.36
Glu120	4.15	0.16	0.01	0.29	0.20
Gly121	7.71	0.26	0.01	1.67	-0.28
His124	9.14	0.30	0.01	2.99	N/A
Val136	2.44	0.12	0.01	0.34	-0.07
Asp144	3.46	0.15	0.01	0.30	0.24
Asn147	3.62	0.15	0.01	0.43	0.14
Ser148	3.75	0.15	0.01	0.33	-0.19
His149	5.23	0.19	0.01	0.27	0.15
Cys152	2.20	0.11	0.01	0.36	0.07

Table S6. Fitted values of R_{ex} (at 18.8 T) and $|\Delta\omega_N|$ for amide ^{15}N probes in the L28F E:THF:NADPH complex. Residues with R_{ex} smaller than 2 s^{-1} are omitted. The X^2 per degree of freedom (DoF) is calculated from the combined fit of ^{15}N and ^{1}H amide dispersion curves to the global k_{ex} and p_b, except for Gly95 where only ^{15}N data are available. The equilibrium shift difference $\Delta\delta_N$ is calculated as the difference in ^{15}N chemical shift between the L28F E:THF:NADPH and L28F E:NADPH complexes. The ^{15}N and ^{1}H resonances of Ile14 have not been assigned for the L28F E:NADPH complex, hence $\Delta\delta_N$ is unavailable for that residue.

Residue	R_{ex} (s^{-1})	$\|\Delta\omega_N\|$ (ppm)	error (ppm)	sign	X^2/DoF	$\Delta\delta_N$ (ppm)
Ala7	15.75	2.77	0.07	ND	1.53	-3.42
Leu8	15.81	2.80	0.07	ND	1.94	1.50
Ile14	12.96	2.05	0.05	+	1.29	N/A
Gly15	8.74	1.39	0.04	+	2.60	0.63
Ala19	8.81	1.40	0.03	+	0.46	1.92
Asn23	10.52	1.64	0.05	+	0.63	1.66
Ala26	7.51	1.23	0.03	-	0.27	-1.41
Ala29	10.76	1.67	0.04	+	0.79	0.41
Trp30	11.00	1.71	0.05	+	0.94	1.71
Phe31	5.95	1.04	0.04	+	0.53	1.18
Lys32	15.71	2.76	0.06	+	1.04	1.87
Arg33	8.11	1.31	0.03	+	0.52	0.97
Asn34	2.51	0.62	0.05	-	1.07	0.11
Thr35	7.84	1.27	0.04	+	1.08	1.03
Val40	16.06	2.89	0.07	ND	2.32	2.76
Arg52	7.95	1.29	0.03	ND	1.64	-0.37
Arg57	10.05	1.57	0.04	+	0.24	1.26
Asn59	11.05	1.72	0.04	+	0.61	1.26
Ala83	2.51	0.62	0.04	+	0.39	0.34
Asp87	5.86	1.03	0.05	+	0.22	0.15
Val93	9.97	1.55	0.03	ND	0.49	-0.98
Gly95	12.92	2.05	0.05	ND	1.81	1.57
Leu104	2.13	0.57	0.04	ND	0.31	0.02
Gln108	2.01	0.55	0.04	ND	0.22	-0.54
Tyr111	5.00	0.93	0.03	ND	0.32	-0.60
Leu112	7.61	1.24	0.03	+	0.25	1.01
His114	5.12	0.95	0.04	ND	1.22	0.61
Ile115	8.04	1.30	0.03	ND	0.68	1.34
Asp116	7.26	1.20	0.03	-	1.70	-0.90
Ala117	8.07	1.30	0.03	+	0.48	1.09
Glu118	2.91	0.67	0.04	ND	0.56	-0.45
Glu120	13.81	2.23	0.06	+	1.13	1.96
Gly121	17.75	3.71	0.08	ND	1.62	3.91
His124	19.80	6.36	0.20	ND	1.05	-5.91
Ser138	3.08	0.69	0.04	ND	0.32	-0.02
Ser148	4.90	0.92	0.04	+	0.20	0.67
His149	14.49	2.40	0.05	ND	1.49	2.78
Ser150	6.38	1.09	0.03	ND	0.57	-1.12

Table S7. Fitted values of R_{ex} (at 18.8 T, 800 MHz) and $|\Delta\omega_H|$ for amide ^1H probes in the L28F E:THF:NADPH complex. Residues with R_{ex} smaller than 2 s^{-1} are omitted. The X^2 per degree of freedom (DoF) is calculated from the combined fit of ^{15}N and ^1H amide dispersion curves to the global k_{ex} and p_b. The equilibrium shift difference $\Delta\delta_H$ is calculated as the difference in proton chemical shift between the L28F E:THF:NADPH and L28F E:NADPH complexes. The ^{15}N and ^1H resonances of Ile14 have not been assigned for the L28F E:NADPH complex, hence $\Delta\delta_H$ is not available for that residue.

Residue	R_{ex} (s^{-1})	$\|\Delta\omega_H\|$ (ppm)	error (ppm)	X^2/DoF	$\|\Delta\delta_H\|$ (ppm)
Ile2	5.88	0.105	0.005	0.33	0.12
Ser3	6.32	0.110	0.005	0.34	0.08
Leu4	2.89	0.068	0.004	0.21	0.03
Ala7	20.76	1.42	0.06	1.53	-1.89
Leu8	10.24	0.161	0.004	1.94	-0.08
Ile14	19.35	0.55	0.02	1.29	N/A
Gly15	20.84	1.70	0.08	2.60	1.54
Ala19	10.72	0.17	0.01	0.46	0.17
Asn23	19.67	0.61	0.03	0.63	0.59
Ala26	15.24	0.26	0.01	0.27	-0.16
Ala29	17.80	0.38	0.02	0.79	0.26
Trp30	17.98	0.39	0.02	0.94	0.54
Phe31	17.20	0.34	0.01	0.53	0.38
Lys32	18.16	0.41	0.02	1.04	0.51
Arg33	19.80	0.65	0.02	0.52	0.51
Asn34	15.20	0.26	0.01	1.07	0.26
Thr35	10.84	0.17	0.01	1.08	0.13
Lys38	16.06	0.29	0.01	0.52	0.28
Val40	17.78	0.38	0.01	2.32	0.27
Arg44	2.83	0.07	0.01	0.23	0.00
Ser49	5.53	0.101	0.004	0.49	0.05
Gly51	10.22	0.161	0.005	0.76	-0.01
Arg52	9.84	0.156	0.004	1.64	0.02
Leu54	18.94	0.48	0.02	1.27	-0.36
Arg57	15.79	0.28	0.01	0.24	0.07
Lys58	20.21	0.80	0.02	0.81	-0.50
Asn59	15.78	0.28	0.01	0.61	0.15
Ile61	2.96	0.069	0.005	0.84	0.03
Leu62	10.28	0.16	0.01	0.76	0.09
Ser64	4.07	0.08	0.01	0.56	-0.01
Asp69	3.92	0.08	0.01	0.36	-0.01
Arg71	5.43	0.100	0.005	0.25	-0.03
Val72	3.63	0.077	0.004	0.97	-0.02
Trp74	2.48	0.062	0.005	1.04	0.02
Val75	5.19	0.097	0.004	0.23	0.05
Val78	2.97	0.07	0.01	0.25	0.04
Glu80	3.13	0.07	0.01	0.30	0.03
Ala81	6.51	0.112	0.005	0.35	0.05
Ile82	10.55	0.17	0.01	0.33	0.09

Ala83	4.23	0.08	0.01	0.39	0.06
Cys85	2.99	0.07	0.01	0.21	0.04
Gly86	4.02	0.082	0.004	2.92	-0.03
Asp87	7.92	0.13	0.01	0.22	0.03
Glu90	7.76	0.128	0.004	0.41	0.11
Ile91	2.53	0.06	0.01	3.27	0.02
Met92	11.59	0.18	0.01	0.75	0.10
Val93	4.02	0.082	0.005	0.49	0.00
Ile94	13.35	0.22	0.01	0.46	0.21
Gln102	4.83	0.092	0.004	0.45	0.04
Leu104	2.86	0.07	0.01	0.31	0.04
Lys106	2.39	0.06	0.01	0.48	0.00
Gln108	4.79	0.09	0.01	0.22	0.00
Leu110	8.47	0.14	0.01	0.54	0.08
Tyr111	5.40	0.10	0.01	0.32	0.00
Leu112	11.97	0.19	0.01	0.25	0.10
Thr113	4.02	0.08	0.01	0.54	0.06
His114	4.08	0.08	0.01	1.22	-0.01
Ile115	8.92	0.14	0.01	0.68	0.08
Asp116	15.95	0.29	0.01	1.70	-0.22
Ala117	18.09	0.40	0.01	0.48	0.38
Glu118	10.21	0.16	0.01	0.56	0.12
Glu120	14.64	0.25	0.01	1.13	0.21
Gly121	17.25	0.35	0.01	1.62	-0.32
His124	19.86	0.66	0.02	1.05	-0.67
Val136	3.12	0.07	0.01	0.24	-0.02
Ser138	3.34	0.074	0.005	0.32	-0.07
Phe140	3.20	0.072	0.005	0.91	-0.04
Asp144	2.02	0.056	0.005	0.41	0.01
Gln146	8.89	0.14	0.01	0.52	0.10
Asn147	11.88	0.19	0.01	0.39	0.16
Ser148	16.67	0.32	0.01	0.20	-0.30
His149	16.6	0.31	0.01	1.49	0.27
Ser150	2.34	0.06	0.01	0.57	-0.02
Cys152	2.34	0.06	0.01	0.31	0.04
Glu154	3.19	0.07	0.01	0.43	0.05

Table S8. Fitted values of R_{ex} (at 18.8 T) and $|\Delta\omega_N|$ for amide ^{15}N probes in the L28F E:THF:$NADP^+$ complex. Residues with R_{ex} smaller than 2 s^{-1} are omitted. The X^2 per degree of freedom (DoF) is calculated from the combined fit of ^{15}N and ^1H amide dispersion curves to the global k_{ex} and p_b, except for Gly95 where only ^{15}N data are available. The equilibrium shift difference $\Delta\delta_N$ is calculated as the difference in ^{15}N chemical shift between the L28F E:THF:$NADP^+$ and L28F E:FOL:$NADP^+$ complexes. The ^{15}N and ^1H resonances of Ala7, Ile14 and His124 have not been assigned for the L28F E:FOL:$NADP^+$ complex, hence $\Delta\delta_N$ is not available for these residues.

Residue	R_{ex} (s^{-1})	$\|\Delta\omega_N\|$ (ppm)	error (ppm)	sign	X^2/DoF	$\Delta\delta_N$ (ppm)
Ala7	6.77	1.21	0.04	ND	1.51	N/A
Leu8	8.08	1.37	0.04	ND	1.11	0.56
Ile14	18.22	3.25	0.08	+	1.67	N/A
Gly15	17.79	3.11	0.08	-	10.12	-2.98
Ala19	8.04	1.36	0.03	ND	0.48	0.58
Asn23	8.66	1.44	0.04	+	0.89	0.98
Leu24	17.48	3.02	0.06	ND	1.22	-2.09
Ala26	4.45	0.93	0.04	-	0.35	-0.24
Asp27	5.85	1.10	0.03	ND	1.23	0.99
Ala29	4.83	0.97	0.04	ND	0.70	0.11
Trp30	4.79	0.97	0.04	+	0.58	0.39
Phe31	6.59	1.19	0.03	ND	1.28	0.49
Lys32	6.04	1.12	0.04	+	1.19	-0.32
Arg33	2.92	0.73	0.04	+	0.72	0.22
Thr35	3.42	0.80	0.05	+	1.13	0.18
Leu36	5.57	1.07	0.04	-	1.27	0.23
Asn37	3.17	0.76	0.04	ND	1.67	0.48
Val40	12.56	1.98	0.04	ND	0.63	1.58
Arg44	2.44	0.66	0.04	ND	0.55	-0.30
Gly51	2.08	0.60	0.04	ND	1.71	0.65
Arg52	5.64	1.07	0.03	+	0.78	0.40
Leu54	2.59	0.68	0.04	ND	1.17	0.23
Arg57	3.02	0.74	0.03	ND	0.30	-0.05
Asn59	3.52	0.81	0.06	ND	0.59	-0.06
Asp87	6.49	1.18	0.04	ND	0.97	0.05
Val93	6.63	1.19	0.03	ND	1.21	-0.65
Gly95	10.14	1.63	0.03	ND	2.16	1.40
Leu104	2.30	0.64	0.04	ND	0.76	-0.06
Gln108	2.20	0.62	0.05	ND	0.44	-0.35
Tyr111	4.05	0.88	0.03	ND	0.63	-0.58
Leu112	4.82	0.97	0.03	ND	0.67	0.00
Ile115	3.55	0.81	0.03	ND	1.27	0.51
Asp116	6.31	1.15	0.03	-	1.93	-0.98
Ala117	7.96	1.35	0.03	+	0.74	0.98
Glu118	5.72	1.08	0.03	ND	0.55	-1.20
Val119	18.84	3.48	0.09	ND	4.95	4.64
Glu120	11.94	1.88	0.05	+	0.86	1.84
Gly121	18.94	3.52	0.07	ND	0.88	3.66

His124	20.65	4.41	0.14	ND	4.54	N/A
Phe140	2.00	0.59	0.04	ND	1.37	-0.43
Ser148	3.49	0.80	0.04	+	0.52	0.39
His149	14.91	2.39	0.05	ND	0.61	1.95
Ser150	3.98	0.87	0.03	ND	0.80	-0.53

Table S9. Fitted values of R_{ex} (at 18.8 T, 800 MHz) and $|\Delta\omega_H|$ for amide ^1H probes in the L28F E:THF:NADP$^+$ complex. Residues with R_{ex} smaller than 2 s^{-1} are omitted. The X^2 per degree of freedom (DoF) is calculated from the combined fit of ^{15}N and ^1H amide dispersion curves to the global k_{ex} and p_b. The equilibrium shift difference $\Delta\delta_H$ is calculated as the difference in proton chemical shift between the L28F E:THF:NADP$^+$ and L28F E:FOL:NADP$^+$ complexes. The ^{15}N and ^1H resonances of Ile14 have not been assigned for the L28F E:FOL:NADP$^+$ complex, hence $\Delta\delta_H$ is unavailable for that residue.

Residue	R_{ex} (s^{-1})	$\|\Delta\omega_H\|$ (ppm)	error (ppm)	X^2/DoF	$\|\Delta\delta_H\|$ (ppm)
Ile2	3.25	0.078	0.007	0.42	-0.01
Ser3	2.70	0.071	0.005	0.65	0.01
Leu4	3.80	0.086	0.004	0.53	-0.09
Ala7	23.64	1.06	0.05	1.51	N/A
Leu8	14.67	0.238	0.007	1.11	-0.13
Ile14	22.39	0.63	0.03	1.67	N/A
Gly15	23.75	1.14	0.10	10.12	1.26
Ala19	7.84	0.136	0.004	0.48	0.03
Asn23	19.39	0.38	0.02	0.89	0.41
Leu24	10.02	0.164	0.005	1.22	-0.10
Ala26	13.50	0.216	0.006	0.35	-0.10
Asp27	6.04	0.114	0.005	1.23	0.03
Ala29	12.32	0.197	0.005	0.70	0.13
Trp30	13.23	0.211	0.007	0.58	0.20
Phe31	17.52	0.31	0.01	1.28	0.34
Lys32	17.72	0.313	0.009	1.19	0.17
Arg33	10.95	0.176	0.006	0.72	0.19
Asn34	11.02	0.177	0.005	1.15	0.14
Thr35	8.26	0.141	0.007	1.13	0.09
Leu36	15.91	0.264	0.009	1.27	0.15
Asn37	15.12	0.247	0.008	1.67	-0.02
Lys38	5.27	0.104	0.004	0.42	-0.05
Val40	4.54	0.095	0.005	0.63	0.00
Arg44	4.02	0.088	0.006	0.55	-0.04
Ser49	9.76	0.160	0.005	2.76	-0.04
Gly51	9.60	0.158	0.004	1.71	0.16
Arg52	14.83	0.241	0.005	0.78	0.09
Leu54	9.62	0.158	0.005	1.17	-0.07
Arg57	4.46	0.094	0.004	0.30	0.02
Lys58	10.36	0.168	0.004	0.78	0.00
Asn59	4.34	0.093	0.007	0.59	-0.06
Ile61	2.30	0.065	0.005	1.46	-0.03
Leu62	4.35	0.093	0.004	0.72	-0.10
Ser63	3.55	0.082	0.005	0.47	-0.05
Ser64	3.94	0.087	0.008	0.39	-0.03
Gln65	2.23	0.063	0.007	0.61	0.00
Asp69	4.68	0.097	0.008	0.49	0.03
Arg71	4.18	0.091	0.005	0.34	0.02
Val72	3.44	0.081	0.005	1.14	-0.03
Thr73	14.17	0.228	0.005	0.33	-0.03

Val75	2.72	0.071	0.003	0.42	0.00
Ile82	3.65	0.084	0.006	0.51	0.01
Asp87	9.37	0.155	0.006	0.97	-0.01
Glu90	4.18	0.091	0.004	0.44	0.02
Met92	8.80	0.148	0.003	1.17	0.13
Val93	14.37	0.232	0.006	1.21	-0.12
Leu104	7.81	0.135	0.004	0.76	0.12
Lys106	2.16	0.062	0.007	1.11	-0.02
Gln108	4.64	0.096	0.005	0.44	0.02
Leu110	5.17	0.103	0.004	0.76	0.00
Tyr111	5.47	0.107	0.005	0.63	-0.12
Leu112	9.23	0.153	0.004	0.67	0.12
Thr113	12.85	0.205	0.005	0.85	-0.18
His114	7.12	0.127	0.005	1.41	0.03
Ile115	8.82	0.148	0.005	1.27	0.01
Asp116	13.96	0.224	0.005	1.93	-0.20
Ala117	19.15	0.37	0.01	0.74	0.37
Glu118	6.98	0.125	0.004	0.55	0.04
Val119	20.05	0.41	0.01	4.95	0.53
Glu120	12.58	0.201	0.006	0.86	0.19
Gly121	17.27	0.299	0.007	0.88	-0.29
His124	22.93	0.748	0.026	4.54	N/A
Val136	5.46	0.107	0.004	0.40	-0.07
Asp142	2.54	0.068	0.004	0.59	0.04
Ala143	2.93	0.074	0.004	1.29	-0.05
Asp144	4.62	0.096	0.003	0.54	0.19
Asn147	11.55	0.185	0.006	0.27	0.17
Ser148	16.52	0.279	0.009	0.52	-0.32
His149	15.24	0.249	0.006	0.61	0.15
Cys152	8.60	0.145	0.005	0.57	0.13
Glu154	4.65	0.096	0.004	0.66	0.04

Table S10. Populations of species present under NMR conditions (18 mM THF, 10 mM NADP(H)), obtained by simulation of the kinetic scheme of Figure 6 for dissociation of THF from E:THF:NADPH and E:THF:NADP+. Rate constants from Tables 2 and 3 were used, together with the THF association rates measured in MTEN buffer at pH 6 (Fierke, C. A.; Johnson, K. A.; Benkovic, S. J. *Biochemistry* **1987**, *26*, 4085.)

	populations			
Complex	^{occ}E:T:N(H)	^{cl}E:T:N(H)	^{occ}E:N(H)	^{cl}E:N(H)
WT E:THF:NADPH	99.3	0.69	< 0.001	0.022
WT E:THF:NADP$^+$	98.7	1.25	< 0.001	< 0.001